AGU PUBLICATIONS

Geophysical Research Letters

RESEARCH LETTER

10.1002/2016GL070918

Key Points:

- The Northern Appalachian Anomaly is an intense low-velocity anomaly in the asthenosphere just east of the cratonic margin
- Its seismic attributes are consistent with a modern thermal origin related to small-scale upwelling at the continental margin
- Its spatial association with the Great Meteor hot spot track is coincidental

Supporting Information:

- Supporting Information S1

Correspondence to:
W. Menke,
menke@ldeo.columbia.edu

Citation:
Menke, W., P. Skryzalin, V. Levin, T. Harper, F. Darbyshire, and T. Dong (2016), The Northern Appalachian Anomaly: A modern asthenospheric upwelling, *Geophys. Res. Lett.*, *43*, doi:10.1002/2016GL070918.

Received 19 AUG 2016
Accepted 28 SEP 2016
Accepted article online 29 SEP 2016

The Northern Appalachian Anomaly: A modern asthenospheric upwelling

William Menke[1], Peter Skryzalin[2], Vadim Levin[2], Thomas Harper[3], Fiona Darbyshire[4], and Ted Dong[1]

[1]Lamont-Doherty Earth Observatory, Columbia University, Palisades, New York, USA, [2]Department of Earth and Planetary Science, State University of New Jersey Rutgers, Piscataway, New Jersey, USA, [3]Department of Geosciences, Boise State University, Boise, Idaho, USA, [4]Centre GEOTOP, Université du Québec à Montréal, Montréal, Québec, Canada

Abstract The Northern Appalachian Anomaly (NAA) is an intense, laterally localized (400 km diameter) low-velocity anomaly centered in the asthenosphere beneath southern New England. Its maximum shear velocity contrast, at 200 km depth, is about 10%, and its compressional-to-shear velocity perturbation ratio is about unity, values compatible with it being a modern thermal anomaly. Although centered close to the track of the Great Meteor hot spot, it is not elongated parallel to it and does not crosscut the cratonic margin. In contrast to previous explanations, we argue that the NAA's spatial association with the hot spot track is coincidental and that it is caused by small-scale upwelling associated with an eddy in the asthenospheric flow field at the continental margin. That the NAA is just one of several low-velocity features along the eastern margin of North America suggests that this process may be globally ubiquitous.

1. Introduction

The eastern North American coast is the site of significant seismic velocity heterogeneities [*Levin et al*., 1995; *Levin et al*., 2000; *Li et al*., 2003; *Godey et al*., 2004; *Nettles and Dziewonski*, 2008; *Chu et al*., 2013; *Schmandt and Lin*, 2014; *Skryzalin et al*., 2015; *Pollitz and Mooney*, 2016; *Porter et al*., 2016]. They are a record—albeit an ambiguous one—of lithospheric and asthenospheric processes operating at the continental margin. We focus on the Northern Appalachian Anomaly (NAA), a particularly strong low-velocity feature in the shallow mantle located in a westward indentation (or divot [*Fouch et al*., 2000]) of the continental lithosphere in southern New England (Figure 1a). The NAA has been explained as a relic feature associated with the Great Meteor hot spot (GMHS) [*van der Lee and Nolet*, 1997; *Eaton and Frederiksen*, 2007] which traversed southern New England at ~130–100 Ma [*Sleep*, 1990]. Here we consider the alternative hypothesis that it is a modern feature associated with small-scale asthenospheric upwelling unrelated to any hot spot. We show that the NAA is a compact (400 km wide) columnar feature and that its traveltime delays are consistent with an extremely strong (~700°C) asthenospheric temperature anomaly. After analyzing several previously published tomographic images and a new one described here, we conclude that it is most consistent with a strong local upwelling associated with the eastern edge of the Laurentian (pre-Cambrian) continental lithosphere [*King and Anderson*, 1998].

Early images of the NAA depict it as having a large (>1000 km) and strongly elongated planform that crosscuts the continental margin [*van der Lee and Nolet*, 1997]. The most recent images [*Schmandt and Lin*, 2014; *Porter et al*., 2016] including our own (Figure 1b), which are based on much denser data coverage, depict it as having a smaller (~400 km) and more subcircular planform positioned just east of the Appalachian Front (AF) [*Hynes and Rivers*, 2010], which itself may be near the eastern edge of the Laurentian lithosphere [*Thomas*, 2006]. The early images are suggestive of GMHS affinity, but the more recent ones are not.

2. Data Analysis

Our new analysis, used to better define the properties of the NAA, is based on broadband digital recordings of $M_w > 5.5$ teleseisms for the 2010–2016 time period from 214 sites (see supporting information Text S1) in New England and southern Canada. Differential *P* and *S* wave traveltimes, relative to the AK135 global model [*Kennett et al*., 1995], were determined for all stations pairs that recorded a given teleseism via cross correlation [e.g., *Menke and Menke*, 2016]. Results were refined with the out-member averaging noise-reduction algorithm [*Menke and Menke*, 2014] (supporting information Text S2).

10.1002/2016GL070918

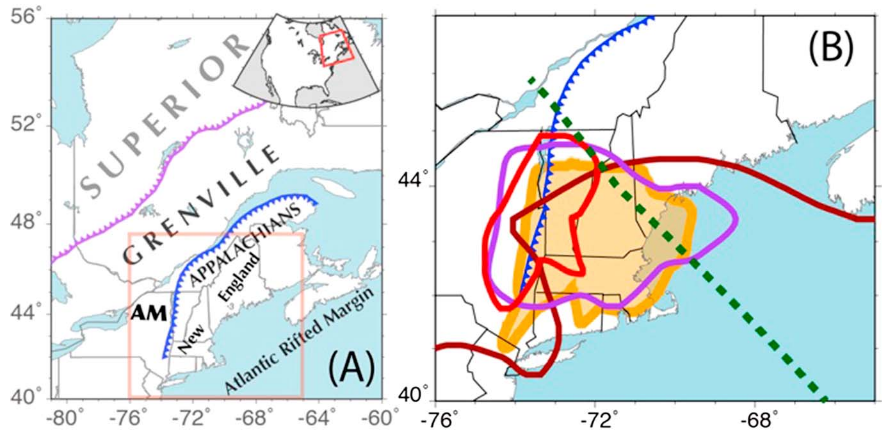

Figure 1. (a) Map of northeastern North America showing the major geological features, including AF (sawtooth blue), Grenville Front (sawtooth purple), and Adirondack Mountains (AM). (b) Enlargement of region (orange box in Figure 1a), showing GMHS track (dashed green) and outline of NAA slow velocity anomaly at 200 km depth by this (orange) and other recent studies (*van der Lee and Nolet* [1997], brown; *Schmandt and Lin* [2014], purple; *Pollitz and Mooney* [2016], red). In all cases, the western end of the NAA is near the AF.

The traveltime anomalies are a measure of the overall heterogeneity of the region. The RMS values are 0.34 s for *P* waves and 0.97 s for *S* waves, with an overall respective range of 2.3 s and 6.8 s (Figure 2a). We put these numbers into context by considering that the 6.8 s *S* traveltime anomaly could be caused by a hypothetical velocity perturbation $\Delta v_S \approx 0.48$ km/s in an upper mantle column with an average shear velocity of 4.6 km/s that is 300 km thick (supporting information Text S3). This ~10% velocity anomaly is surprisingly large for a

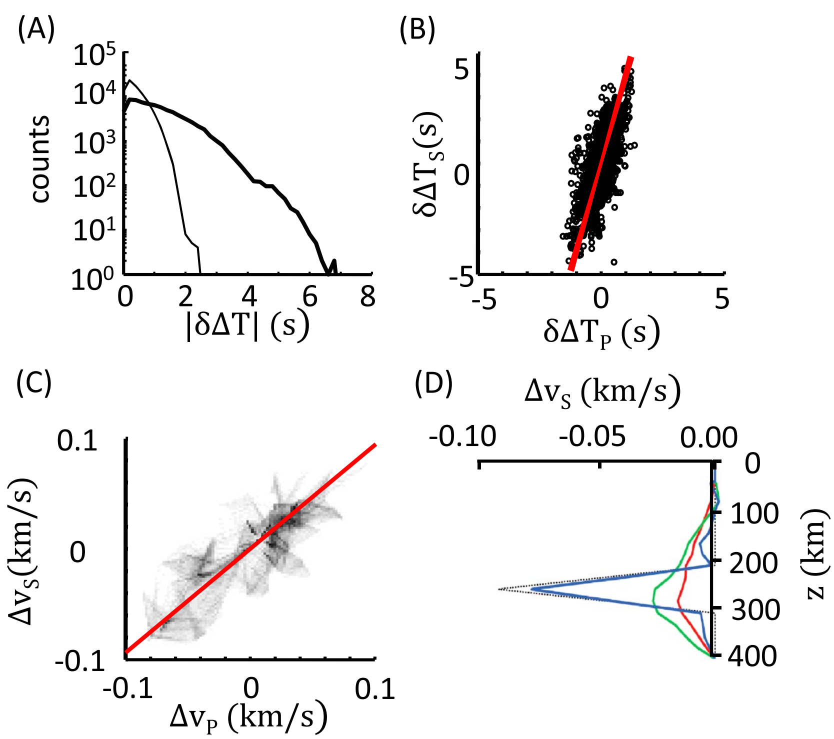

Figure 2. (a) Histograms of *P* wave (solid) and *S* wave (bold) differential traveltime anomalies $\delta\Delta T$ (relative to the AK135 prediction). Only delays from pairs of stations observing the same teleseism are counted. (b) Scatterplot of $\delta\Delta T_P$ versus $\delta\Delta T_S$ for the same data described in Figure 2a, with best fitting line (red). (c) Scatterplot of Δv_P versus Δv_S for slice through tomographic model at 200 km depth, with best fitting line (red). (d) Resolution test showing vertical profile through a hypothetical slow anomaly (grey) centered at 250 km depth, and three recovered anomalies (blue, red, and green) for different amounts of damping (supporting information Texts S4 and S5).

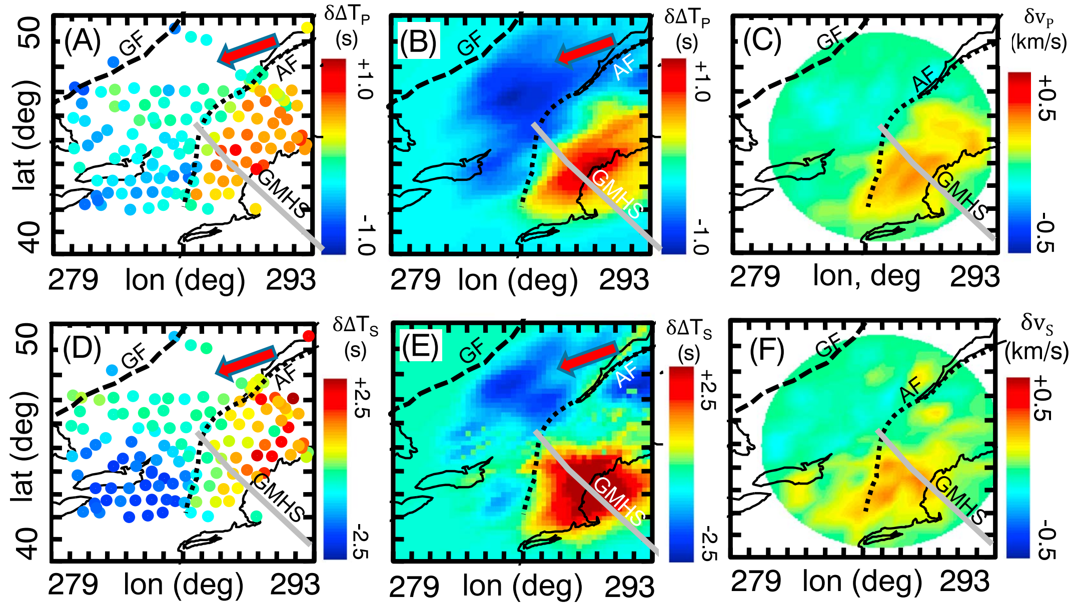

Figure 3. (a) *P* wave traveltime anomalies for a teleseism from the west (red arrow, which points back toward the hypocenter) observed at seismic stations (circles). AF, GF, and GMHS track are also shown. (b) *P* wave traveltime anomalies predicted by the tomographic model in Figure 3c. (c) Slice through v_P tomogtaphic model at 100 km depth, with regions further than 500 km from the array center masked to reflect ray coverage. (d–f) Same as Figures 3a–3c but for *S* wave. The latest traveltime anomalies and slowest velocities occur east of the AF.

nominally tectonically quiescent region. Both *P* wave and *S* wave traveltime anomalies exhibit spatially coherent structure that is dominated by fast arrivals in the cratonic northwest of the study region and late arrivals in a region that is centered in southern New England (the NAA; Figures 3a and 3b). The boundary between fast and slow regions is sharp and roughly follows the AF.

We invert differential traveltime anomalies for three-dimensional compressional and shear wave structure using RAYTRACE3D [*Menke*, 2005; see also *Menke*, 2012] (supporting information Text S4). The inversions (Figures 3c and 3f) indicate that the NAA is predominantly an asthenospheric feature, being most intense at and below 100 km depth. It has a columnar shape that varies only slowly with depth. The most intense core of the anomaly may plunge ~25° with respect to the vertical to the southwest. Resolution tests (Figure 2d and supporting information Text S5) indicate that the data are adequate to resolve the anomaly's base, where such a feature is present in the ~250–300 km range, yet it is not imaged in our inversion. The NAA is centered in southern New Hampshire (N42.8, 72.2°W) and is ~400 km wide, measured perpendicular to the continental margin, and is somewhat elongated in the margin-parallel direction. The peak-to-peak range in v_S anomalies in the region is ~9.8%, which agrees with the rough estimate derived previously.

The *S* wave and *P* wave traveltime anomalies are highly correlated, with $(\delta\Delta t)_S/(\delta\Delta t)_P = 3.98 \pm 0.26$ (95 %) (Figure 2b and supporting information Text S6). If we assume these anomalies arise from compressional and shear velocity heterogeneities Δv_S and Δv_P around the background velocities of $v_{0S} = 4.52$ km/s and $v_{0P} = 8.30$ km/s given by AK135 for 210 km depth, then (supporting information Text S6)

$$\frac{\Delta v_S}{\Delta v_P} = \frac{(\delta\Delta t)_S}{(\delta\Delta t)_P}\left(\frac{v_{0P}}{v_{0S}}\right)^{-2} = 1.18\pm0.08\ (95\%)$$

This ratio can be compared to the results of inversions, though with caution, since those results depend upon the values of the damping parameters, the distribution of rays and upon depth. *Schmandt and Lin's* [2014] model yields $\Delta v_S/\Delta v_P = 1.00 \pm 0.10$ (95 %) at 195 km depth (supporting information Text S6). When the damping parameters in our inversions are chosen so that the *P* and *S* error reduction is equal, they yield the similar value of 0.96 ± 0.02 (95 %) at 200 km depth (Figure 2c).

3. Discussion

The tectonic inheritance model [*Thomas*, 2006] suggests that the AF is just west of the eastern edge of Laurentia. The juxtaposition of the AF and the western edge of the NAA indicate that at shallow mantle depths, the emplacement of the NAA was guided by the eastern edge of the Laurentian lithosphere and does not crosscut it.

The observed perturbations in compressional and shear velocity across the NAA are very intense, comparable to the difference in shallow mantle shear velocities between tectonically quiescent cratonic North America and the tectonically active Basin and Range province [*Nettles and Dziewonski*, 2008]. This latter velocity contrast is thought to be caused by the ~700°C temperature contrast between extremely hot partially molten Basin and Range asthenosphere, with temperature as hot [*Plank and Forsyth*, 2016] as ~1550–1600°C (at 100 km depth) and cold [*Hasterok and Chapman*, 2011] (~850–900°C at 100 km depth) lithosphere beneath the craton. The observed 6.8 s traveltime anomaly could be caused by 770°C ± 180°C temperature anomaly, according to a recent model [*Cammarano et al*., 2003] of velocity-temperature derivatives (supporting information Text S7).

A thermal anomaly perturbs both compressional and shear velocity. However, modeling the thermally induced $\Delta V_S/\Delta V_P = [dV_S/d\theta]/[dV_P/d\theta]$ in the upper mantle is complicated by the need to correct laboratory measurements for the effects of pressure, anelasticity, partial melt, etc. A recent model [*Cammarano et al*., 2003] predicts $\Delta V_S/\Delta V_P = 0.97$ at 200 km depth along a 1300°C adiabat (supporting information Text S8). The good agreement between this prediction and our estimates implies that the observed velocity ratios are consistent with a thermal origin. Furthermore, the observed velocity ratio rules out some other mechanisms, including fluctuations in the Fe/Mg ratio of mantle minerals (supporting information Text S8).

Monte Carlo simulations [*Levin et al*., 1996] indicate that the scaling between shear wave splitting times and *P* wave traveltime anomalies is about 1 to ±0.3, when both are caused by lateral variations in upper mantle anisotropy. This scaling implies that the observed ±1.15 s fluctuation (Figure 2a) in *P* wave traveltime should be accompanied by about 3.8 s of *SKS* splitting. In contrast, observed splitting delays rarely exceed 1 s in New England [*Levin et al*., 2000; *Long et al*., 2016]. Anisotropy therefore can make only a minor (<25%) contribution to the NAA's traveltime anomaly.

Excess Helium-3 is generally considered a proxy for active volcanism and extension when it occurs in continental settings. Its presence in the groundwater of southern New England [*Torgersen et al*., 1995] is anomalous and has prompted explanations involving storage and slow release of mantle helium from an ancient source such as the GMHS [*Torgersen et al*., 1995]. This excess helium is better explained by modern mantle upwelling.

Several asthenospheric flow scenarios plausibly could have caused the NAA: Large-scale flow of the asthenosphere past the west deepening lithospheric keel of the continent could induce eddies that drive small-scale convective upwelling [*King and Ritsema*, 2000]. Large-scale flow of the asthenosphere also could entrain and laterally transport anomalously hot asthenosphere that was formed elsewhere (e.g., from a distant plume [*Phipps Morgan et al*., 1995]). Delamination of the continental lithosphere could lead to local upwelling of the asthenosphere to fill in the gap made by cold, sinking material [*Boyd et al*., 2004]. The available data do not rule out any of these mechanisms, yet our analysis is most consistent with the first; that is, the NAA is a small-scale cratonic edge-related upwelling. Lateral transport (the second scenario) implies significant shearing and tilting of a hot region, which is not supported by the NAA's columnar shape and vertical orientation. A recent delamination implies the presence of seismically fast material below the NAA and predicts a strong seismic impedance contrast in the lower asthenosphere. No such feature has been observed in receiver functions from southern New England (and especially in the high-quality results from station HRV (Harvard, Massachusetts)) [*Rychert et al*., 2007].

The Missouri to Massachusetts Broadband Seismometer Experiment (MOMA) [*Li et al*., 1998] provides high-resolution estimates of the topography of the 410 km discontinuity across a transect that includes the NAA. Only very slight (<5 km) and statistically insignificant deepening of the discontinuity is detected beneath the NAA in contrast to the ~25 km deflection expected when an upwelling crosses this discontinuity. This null result is consistent with a shallow edge-driven model in which mantle flow lines do not cross into the transition zone.

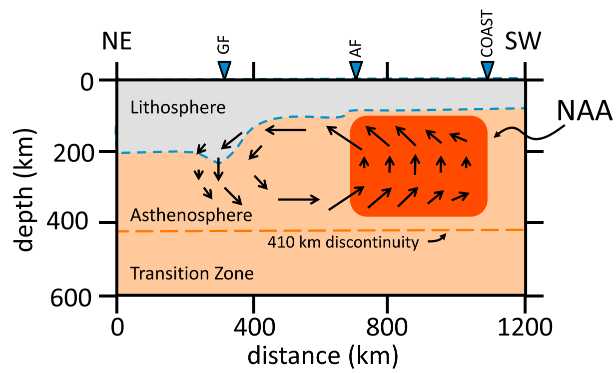

Figure 4. Schematic interpretation of the NAA, informed by *King and Ritsema*'s [2000, Figure 2b] model of edge-driven convection. See text for further discussion.

In our interpretation (Figure 4), the NAA is the upwelling limb of a small-scale convection cell of the type predicted by *King and Ritsema* [2000]. The position and shape of the NAA is strongly constrained by data; the small step in the lithosphere at the AF and the absence of flow beneath the 410 km discontinuity are only weakly constrained. The deformation of the lithosphere by the downwelling at the GF is purely conjectural; future work to detect (or rule out) this feature is warranted,

Flow models based on buoyancy inferred from global seismic tomography [*Forte et al*., 2010; *Levin et al*., 2013] predict subhorizontal flow in the asthenosphere beneath eastern North America, with some downwelling beneath the cold craton. The southwesterly azimuth of this flow is consistent with layered anisotropy models satisfying multiple constraints [*Yuan and Levin*, 2014] and also with the southwesterly plunge of the NAA (which might be caused by mantle shear). However, these flow models appear to be too long wavelength to resolve the kind of small-scale upwelling we propose for the NAA.

Subvertical flow, as we envision for the NAA, might be associated with smaller than normal *SKS* splitting delay times, because seismic anisotropy perpendicular to the *A* axis of olivine, which aligns with flow, is weak. Single-layer interpretations of *SKS* delay times in southern New England [*Long et al*., 2016] do appear to give smaller delays in the vicinity of the NAA than in adjacent areas to the north and west, though the planform does not match its shape in any detail. The difference might be due the interfering effect of lithospheric anisotropy and might be resolved by multilayer interpretations, should they become available.

The NAA has no obvious expression in the Bouguer gravity map of the United States [*Kucks*, 1999], which is dominated by linear features that strike parallel to the Appalachian orogeny and are thought to be related to variations in crustal density and thickness [*Bird and Dewey*, 1970; *Hatcher*, 2010]. Neither does the NAA have an obvious expression in the much longer wavelength GEOID12B geoid map [*Wang*, 2012]. The horizontal position of the NAA is close to the transition between the sedimented southern Appalachians and more deeply eroded metamorphic northern Appalachians that *Crough* [1981] proposed to be related to uplift associated with the passage of the GMHS. A link to edge-driven uplift is in our opinion more plausible because the uplift in northern New England is far from the GMHS track but plausibly nearby other now-defunct NAA-like upwellings that might have occurred farther north along the cratonic margin during the last 100 Ma. However, this speculation lacks corroborating data.

Notwithstanding our interpretation of the NAA as due to present-day mantle upwelling and the presence of a Helium-3 anomaly that implies a pathway for volatiles from the NAA to the crust, no Tertiary volcanism or tectonism has been reported in southern New England. The most recent volcanic/plutonic rocks are associated with the passage of the Great Meteor hot spot at about 110–130 Ma and the most recent tectonic event was the uplift of the southeastern Adirondack Mountains at 83–112 Ma [*Roden-Tice et al*., 2000]. One possibility is that the mantle upwelling that emplaced the NAA has not been sufficiently continuous to produce large volumes of melt. An intriguing alternate possibility is that the NAA is an incipient feature that will lead to a magmatic event in a few million years.

4. Conclusions

The Northern Appalachian Anomaly (NAA) is an extremely strong (~10% shear velocity contrast), columnar and laterally localized (400 km diameter) low-velocity anomaly centered in the asthenosphere beneath southern New England. Its shear velocity contrast and, by implication, temperature differential are of similar magnitude to that between the Basin and Range province of western North America and the North American craton. Its strength, together with its $\Delta V_S/\Delta V_P$ ratio of about unity, is compatible with it being a modern thermal anomaly. Although centered close to the track of the Great Meteor hot spot, it is not elongated parallel to it and does not crosscut the cratonic margin. In contrast to previous explanations [*van der Lee and Nolet*, 1997; *Eaton and Frederiksen*, 2007], we believe that the NAA's spatial association with the Great Meteor hot spot track is coincidental. Instead, the evidence is more compatible with the NAA being caused by small-scale upwelling associated with an eddy in the asthenospheric flow field at the continental margin. Furthermore, the NAA is only one of several low-velocity anomalies along the eastern North American margin (albeit the most intense and best studied). The others [*Chu et al*., 2013; *Schmandt and Lin*, 2014] include the Central Appalachian Anomaly (CAA) beneath northern Virginia and as yet unnamed anomalies beneath northern South Carolina and Louisiana. The edge-driven upwelling scenario provides a common explanation for them all; furthermore, it does so in a way that explains why they are all present today and lack the age progression characteristic of a hot spot (such as the GMHS and the one hypothesized by *Chu et al*. [2013]). Edge-driven upwelling is, in our view, more compelling than scenarios tailored to each anomaly, individually, because it implies a process that might be occurring at continental margins worldwide.

Acknowledgments
All seismic data used in this study are publically available through the Incorporated Research Institutions for Seismology (IRIS), except that the QMIII Array data are embargoed through the Fall of 2017, and all hypocentral data through the U.S. Geological Survey. We thank the Maine Geological Survey, Maine Forest Service, Maine Department of Environmental Protection and the many landowners who hosted QMIII seismic stations. This research was supported by the National Science Foundation under grants EAR 11–47742, OCE 13–59194, and EAR 11–47831. Support for P.S. was provided by the Rutgers University Aresty Research Assistant Program.

References

Bird, P., and J. Dewey (1970), Lithosphere plate-continental margin tectonics and the evolution of the Appalachian orogen, *Geol. Soc. Am. Bull*., *81*, 1031–1060, doi:10.1130/0016-7606(1970)81[1031:LPMTAT]2.0.CO;2.

Boyd, O. S., C. H. Jones, and A. F. Sheehan (2004), Foundering lithosphere imaged beneath the Southern Sierra Nevada, California, USA, *Science*, *305*, 660–662, doi:10.1126/science.1099181.

Cammarano, F., S. Goes, P. Vacher, and D. Giardini (2003), Inferring upper-mantle temperatures from seismic velocities, *Phys. Earth Planet. Int*., *138*, 197–222, doi:10.1016/0012-821X(95)00238-8.

Chu, R., W. Leng, D. V. Helmberger, and M. Gurnis (2013), Hidden hotspot track beneath the eastern United States, *Nat. Geosci*., *6*, 963–966, doi:10.1038/ngeo1949.

Crough, S. T. (1981), Mesozoic hotspot epeirogeny in eastern North America, *Geology*, *9*, 2–6, doi:10.1130/0091-7613(1981)9<2:MHEIEN>2.0.CO;2.

Eaton, D. W., and A. Frederiksen (2007), Seismic evidence for convection-driven motion of the North American Plate, *Nature*, *446*, 428–421, doi:10.1038/nature05675.

Forte, A., R. Moucha, N. Simmons, S. Grand, and J. Mitrovica (2010), Deep-mantle contributions to the surface dynamics of the North American continent, *Tectonophysics*, *481*, 3–15, doi:10.1016/j.tecto.2009.06.010.

Fouch, M. J., K. M. Fischer, E. M. Parmentier, M. E. Wysession, and T. J. Clarke (2000), Shear wave splitting, continental keels, and patterns of mantle flow, *J. Geophys. Res*., *105*, 6255–6275, doi:10.1029/1999JB900372.

Godey, S., F. Deschamps, J. Trampert, and R. Snieder (2004), Thermal and compositional anomalies beneath the North American continent, *J. Geophys. Res*., *109*, B01308, doi:10.1029/2002JB002263.

Hasterok, D., and D. S. Chapman (2011), Heat production and geotherms for the continental lithosphere, Earth Planet, *Sci. Lett*., *307*, 59–70, doi:10.1016/j.epsl.2011.04.034.

Hatcher, R. D. (2010), The Appapachian orogen: A brief summary, *Geol. Soc. Am. Mem*., *206*, 1–19, doi:10.1130/2010.1206(01).

Hynes, A., and T. Rivers (2010), Protracted continental collision—Evidence from the Grenville Front, *Canadian J. Earth Sci*., *47*, 591–620, doi:10.1139/E10-003.

Kennett, B. L. N., E. R. Engdahl, and R. Buland (1995), Constraints on seismic velocities in the Earth from travel times, *Geophys. J. Int*., *122*, 108–124, doi:10.1111/j.1365-246X.1995.tb03540.x.

King, S. D., and D. L. Anderson (1998), Edge-driven convection, Earth planet, *Sci. Lett*., *160*, 289–296, doi:10.1016/S0012-821X(98)00089-2.

King, S. D., and J. Ritsema (2000), African hot spot volcanism: Small-scale convection in the upper mantle beneath cratons, *Science*, *10*, 1137–1140, doi:10.1126/science.290.5494.1137.

Kucks, R. P. (1999), Bouguer gravity anomaly data grid for the conterminous US, U.S. Geological Survey. [Available at https://mrdata.usgs.gov/services/gravity/bouguer, Accessed 20 September 2016.]

Levin, V., A. Lerner-Lam, and W. Menke (1995), Anomalous mantle structure at the Proterozoic-Paleozoic boundary in northeasten US, *Geophys. Res. Lett*., *22*, 121–124, doi:10.1029/94GL02693.

Levin, V., W. Menke, and J. Park (2000), No regional anisotropic domains in the northeastern U.S. Appalachians, *J. Geophys. Res*., *105*, 19,029–19,042, doi:10.1029/2000JB900123.

Levin, V., W. Menke, and A. Lerner-Lam (1996), Seismic anisotropy in northeastern US as a source of significant teleseismic *P* traveltime anomalies, *Geophys. J. Int*., *126*, 593–603, doi:10.1111/j.1365-246X.1996.tb05312.x.

Levin, V., R. Moucha, and H. Yuan (2013), Upper mantle texture patterns in eastern North America from seismic anisotropy and global mantle flow calculations American Geophysical Union, Fall Meeting 2013, abstract DI21C-06.

Li, A., K. M. Fischer, M. E. Wysession, and T. J. Clarke (1998), Mantle discontinuities and temperature under the North American continental keel, *Nature*, *395*, 160–163, doi:10.1038/25972.

Li, A., D. W. Forsyth, and K. M. Fischer (2003), Shear velocity structure and azimuthal anisotropy beneath eastern North America from Rayleigh wave inversion, *J. Geophys. Res*., *108*, 2362, doi:10.1029/2002JB002259.

Long, M. D., K. G. Jackson, and J. F. McNamara (2016), *SKS* splitting beneath Transportable Array stations in eastern North America and the signature of past lithospheric deformation, *Geochem. Geophys. Geosyst*., *17*, 2–15, doi:10.1002/2015GC00608.

Menke, W. (2005), Case studies of seismic tomography and earthquake location in a regional context, in *Seismic Earth: Array Analysis of Broadband Seismograms*, *Geophysical Monograph Series 157*, edited by A. Levander and G. Nolet, pp. 7–36, ISBN: 978-0-87590-422-12005 , AGU, Washington D.C.

Menke, W. (2012), *Geophysical Data Analysis: Discrete Inverse Theory*, 3rd ed., 293 pp., Academic Press, (Elsevier), Amsterdam.

Menke, W., and J. Menke (2016), *Environmental Data Analysis With MATLAB*, 2nd ed., pp. 342, Academic Press (Elsevier), Amsterdam.

Menke, W. H., and H. P. Menke (2014), Improved precision of delay times determined through cross correlation achieved by out-member averaging, *Jokull*, *64*, 15–22, ISSN:0449–0576.

Nettles, M., and A. M. Dziewonski (2008), Radially anisotropic shear velocity structure of the upper mantle globally and beneath North America, *J. Geophys. Res.*, *113*, B02303, doi:10.1029/2006JB004819.

Phipps Morgan, J., E. J. Morgan, Y.-S. Zhang, and W. H. F. Smith (1995), Observational hints for a plume-fed, suboceanic asthenosphere and its role in mantle convection, *J. Geophys. Res.*, *100*, 12,753–12,767, doi:10.1029/95JB0004.

Plank, T., and D. W. Forsyth (2016), Thermal structure and melting conditions in the mantle beneath the Basin and Range province from seismology and petrology, *Geochem. Geophys. Geosyst.*, *17*, 1312–1338, doi:10.1002/2015GC006205.

Pollitz, F. F., and W. D. Mooney (2016), Seismic velocity structure of the crust and shallow mantle of the Central and Eastern United States by seismic surface wave imaging, *Geophys. Res. Lett.*, *43*, 118–126, doi:10.1002/2015GL066637.

Porter, R., Y. Liu, and W. E. Holt (2016), Lithospheric records of orogeny within the continental U.S, *Geophys. Res. Lett.*, *43*, 144–153, doi:10.1002/2015GL066950.

Roden-Tice, M. K., S. J. Tice, and I. S. Schofield (2000), Evidence for differential unroofing in the Adirondack Mountains, New York State, determined by apatite fission-track thermochronology, *J. Geology*, *108*, 155–169, doi:10.1086/314395.

Rychert, C. A., S. Rondenay, and K. M. Fischer (2007), *P*-to-*S* and *S*-to-*P* imaging of a sharp lithosphere—Asthenosphere boundary beneath eastern North America, *J. Geophys. Res.*, *112*, B08314, doi:10.1029/2006JB004619.

Schmandt, B., and F.-C. Lin (2014), *P* and *S* wave tomography of the mantle beneath the United States, *Geophys. Res. Lett.*, *41*, 6342–6349, doi:10.1002/2014GL061231.

Skryzalin, P. A., W. H. Menke, T. B. Harper, V. L. Levin, and F. A. Darbyshire (2015), The seismically slow feature in the asthenosphere beneath Southern New England is small and intense, AGU Fall Meeting, Abstract T11B-2886.

Sleep, N. H. (1990), Monteregian hotspot track: A long-lived mantle plume, *J. Geophys. Res.*, *95*, 21,983–21,990, doi:10.1029/JB095iB13p21983.

Thomas, W. A. (2006), Tectonic inheritance at a continental margin, *GSA Today*, *16*, 4–11, doi:10.1130/1052-5173(2006)016<4:TIAACM>2.0.CO;2.

Torgersen, T., S. Drenkard, M. Stute, P. Schlosser, and A. Shapiro (1995), Mantle helium in ground waters of eastern North America: Time and space constraints on sources, *Geology*, *23*, 675–678, doi:10.1130/0091-7613(1995)023<0675:MHIGWO>2.3.CO;2.

van der Lee, S., and G. Nolet (1997), Upper mantle *S* velocity structure of North America, *J. Geophys. Res.*, *102*, 22,815–22,838, doi:10.1029/97JB01168.

Wang, Y. M. (2012), GEIOD12B Geoid Model, National Geodetic Survey. [Available at http://www.ngs.noaa.gov/GEOID/GEOID12B, Accessed 20 September 2016.]

Yuan, H., and V. Levin (2014), Stratified seismic anisotropy and the lithosphere-asthenosphere boundary beneath eastern North America, *J. Geophys. Res. Solid Earth*, *119*, 3096–3114, doi:10.1002/2013JB010785.